Nuclear symmetry energy components and their ratio: A new approach within the coherent density fluctuation model

M. K. Gaidarov,[1] E. Moya de Guerra,[2] A. N. Antonov,[1] I. C. Danchev,[3] P. Sarriguren,[4] and D. N. Kadrev[1]

[1]*Institute for Nuclear Research and Nuclear Energy, Bulgarian Academy of Sciences, Sofia 1784, Bulgaria*

[2]*Grupo de Física Nuclear, Departamento de Estructura de la Materia (EMFTEL), Facultad de Ciencias Físicas, Universidad Complutense de Madrid, E-28040 Madrid, Spain*

[3]*Department of Physical and Mathematical Sciences, School of Arts and Sciences, University of Mount Olive, 652 R.B. Butler Dr., Mount Olive, North Carolina 28365, USA*

[4]*Instituto de Estructura de la Materia, IEM-CSIC, Serrano 123, E-28006 Madrid, Spain*

(Received 31 May 2021; revised 19 August 2021; accepted 30 September 2021; published 11 October 2021)

A different alternative approach to calculate the ratio of the surface to volume components of the nuclear symmetry energy is proposed in the framework of the coherent density fluctuation model (CDFM). An alternate expression (scheme II) for the ratio is derived consistently within the model. This expression appears in a form more direct and physically motivated than the expression (scheme I) that was used in our previous works within the CDFM and avoids preliminary assumptions and mathematical ambiguities in scheme I. The calculations are based on the Skyrme and Brueckner energy-density functionals for nuclear matter and on the nonrelativistic Brueckner-Hartree-Fock method with realistic Bonn B and Bonn CD nucleon-nucleon potentials. The approach is applied to isotopic chains of Ni, Sn, and Pb nuclei using nuclear densities obtained in self-consistent Hartree-Fock+BCS calculations with the SLy4 Skyrme effective interaction. The applicability of both schemes within the CDFM is demonstrated by a comparison of the results with the available empirical data and with results of other theoretical studies of the considered quantities. Although in some instances the results obtained for the studied ratio and the symmetry energy components are rather close in both schemes, the proposed scheme II leads to more realistic values that agree better with the empirical data and exhibits conceptual and operational advantages.

DOI: 10.1103/PhysRevC.104.044312

I. INTRODUCTION

The symmetry energy is a crucial quantity in nuclear physics and its astrophysical applications (see, e.g., Ref. [1]). Also, heavy-ion collisions at intermediate energies are considered as a unique tool to explore the nuclear equation of state (EOS) under laboratory controlled conditions. For instance, the combined experiment at GANIL, where the VAMOS spectrometer was coupled with the 4π INDRA detector to study the isotopic distributions produced in ^{40,48}Ca + ^{40,48}Ca collisions at 35 MeV/nucleon, allowed one to estimate the relative contribution of surface and volume terms to the symmetry energy in the nuclear EOS [2]. The knowledge of this contribution and, especially, the relevance of the surface term are important to explore to what extent one can learn about the density dependence of the symmetry energy in infinite nuclear matter (NM) from multifragmentation of finite nuclei and from nuclear reaction dynamics.

The density dependence of the symmetry energy is fairly unknown and there are very different predictions for the various models (see, for instance, Ref. [3]). It is revealed in the relationship between the basic symmetry energy parameters and the neutron-skin thickness in a heavy nucleus. The latter has an explicit dependence on the slope parameter of the symmetry energy via the density dependence of the surface tension, which has been determined in Ref. [4] within a compressible droplet model. Measurements of nuclear structure characteristics including masses, densities, and collective excitations have resolved some of the basic features of the EOS of nuclear matter. The EOS allows one to constrain the bulk and surface properties of the nuclear energy-density functionals (EDFs) quite effectively via the symmetry energy and related properties. The latter are significant ingredients of the EOS and their study in both asymmetric nuclear matter and finite nuclei are of particular importance.

The symmetry energy of a finite nucleus is a collective feature with volume and surface terms, but it is also related to the nucleon-nucleon (NN) interaction and the energy-density functional. For example, there is an analytical parametrization of the link between the Skyrme (see Ref. [5]) and Brueckner [6,7] EDFs and the symmetry energy (see, e.g., Refs. [5,8]). Additionally, when exploring the symmetry energy properties of neutron-rich nuclei by means of the nonrelativistic Brueckner-Hartree-Fock (BHF) method with modern realistic Bonn B and Bonn CD potentials [9], we performed nuclear matter many-body calculations and then results for finite nuclei were obtained within the coherent density fluctuation model (CDFM) (see, e.g., Refs. [10,11]). The

use of the latter (which will be discussed below and applied in the present work) is closely related to the general point of the proper account for the *NN* correlations. It is known that the short-range and tensor *NN* correlations induce a population of high-momentum components in the many-body nuclear wave function. In Ref. [12] the impact of such high-momentum components on bulk observables associated with isospin asymmetric matter has been studied. It was shown that the kinetic part of the symmetry energy is strongly reduced by correlations when compared with the noninteracting case. The results for nuclear matter obtained in Ref. [13] have confirmed the critical role of the tensor force in the determination of the symmetry energy and its slope parameter even at densities not too far above the saturation density.

The coherent density fluctuation model is a natural extension of the Fermi gas model based on the δ-function limit of the generator coordinate method [11,14] and includes long-range correlations of collective type. The CDFM has been applied to calculate various quantities of nuclear structure and reactions. Here we mention some of them. In Ref. [15], CDFM results for the energies, density distributions, and rms radii of the ground and first monopole states in ^{4}He, ^{16}O, and ^{40}Ca nuclei have been obtained. Also, results for the incompressibility of finite nuclei have been reported in Refs. [11,16]. The CDFM has been employed to calculate the scaling function in nuclei using the relativistic Fermi gas scaling function [17,18] and the result has been applied to lepton scattering processes [17–23]. In particular, the CDFM analyses became useful to obtain information about the role of the nucleon momentum and density distributions for the explanation of superscaling in lepton-nucleus scattering [18,19]. The CDFM scaling function has been used to predict cross sections for several processes: inclusive electron scattering in the quasielastic and Δ regions [20,21] and neutrino (antineutrino) scattering both for charge-changing [21,23] and neutral-current [22,23] processes. The model was applied to study the scaling function and its connection with the spectral function and the momentum distribution [24,25]. The CDFM was used also to study the role of the *NN* correlations in elastic magnetic electron scattering [26–28].

In our previous works [8,9,29–34] we demonstrated the capability of the CDFM to be applied as an alternative way to make a transition from the properties of nuclear matter to the properties of finite nuclei investigating the nuclear symmetry energy (NSE), the neutron pressure, and the asymmetric compressibility in finite nuclei. While there is enough information collected for these key EOS parameters (although the uncertainty of their determination is still large), the volume and surface symmetry energies have been poorly investigated until now. This concerns mostly the surface contribution to the NSE and comes from the fact that many nucleons are present around the nuclear surface. The volume and surface contributions to the NSE and their ratio at zero temperature were calculated in Ref. [31] within the CDFM using two EDFs, namely, the Brueckner and Skyrme EDFs. The CDFM weight function was obtained by means of the proton and neutron densities obtained from the self-consistent deformed Hartree-Fock (HF)+BCS method with density-dependent Skyrme interactions. The results obtained in the cases of Ni, Sn, and Pb isotopic chains were compared with results of other theoretical methods and with those from approaches which used experimental data on binding energies, excitation energies to isobaric analog states (IAS), and neutron-skin thicknesses. An investigation of the thermal evolution of the NSE components and their ratio for isotopes belonging to the same chains around the double-magic nuclei performed in Ref. [32] has extended our previous analysis of these nuclei for temperatures different from zero.

In this paper, we revisit the expression for the ratio between the volume and surface components to the NSE within the CDFM proposed in Refs. [9,31] and suggest an alternative approach in a more direct and physically motivated way to calculate this ratio. The main aim of the work is to avoid the preliminary assumptions and mathematical ambiguities in our previous scheme I. To achieve this goal, in the proposed scheme II, we apply the general relation based on the droplet model between the symmetry energy and its components to the building units ("fluctons") of the CDFM model, and we construct from them the ratio between the NSE components for finite nuclei following the standard CDFM procedure. This provides more solid physical grounds to the proposed scheme, which is expected to lead to more reliable results. We also search for the dependence of the results on several sets of nuclear potentials. In the proposed approach we perform calculations for the symmetry energy components $S^{V}(A)$ and $S^{S}(A)$ and their ratio for the same isotopes in Ni ($A = 74$–84), Sn ($A = 124$–156), and Pb ($A = 202$–214) chains considered before and compare the obtained results with the previous ones [including $S^{V}(A)$, $S^{S}(A)$, and their ratio κ] obtained by the procedure in Refs. [9,31]. The applicability of our both schemes within the CDFM is also demonstrated by a comparison of the results with the available empirical data and with results of other theoretical studies for the considered quantities.

In the next section, we give definitions of the EOS parameters governing its density dependence in nuclear matter and finite nuclei using the CDFM, as well as expressions of various quantities of interest in the previous and proposed alternative approach within the CDFM. Section II A briefly explains the derivation of the expression for the ratio of the volume to the surface symmetry energy coefficients on the basis of the local density approximation to the symmetry energy. Section II B contains the previous CDFM formalism, which provides a way to calculate the mentioned quantities. The proposed alternative approach aiming to calculate the NSE components and their ratio is formulated in Sec. II C. Our numerical results are presented and discussed in Sec. III. The main conclusions of the study are summarized in Sec. IV.

II. THEORETICAL SCHEME

A. Main relationships for equation-of-state parameters in nuclear matter and in finite nuclei

The Bethe-Weizsäcker semi-empirical mass formula describes both properties of symmetric (finite) nuclear matter as well as the essential dependence of the finite nucleus

ground-state energy on the isospin asymmetry (polarization) [35–38]:

$$E(A,Z) = -B + E_S A^{-1/3} + S(A)\frac{(N-Z)^2}{A^2} + E_C\frac{Z^2}{A^{4/3}} + E_{\rm dif}\frac{Z^2}{A^2} + E_{ex}\frac{Z^{4/3}}{A^{4/3}} + a\Delta A^{-3/2}. \quad (1)$$

In Eq. (1) $B \simeq 16$ MeV is the binding energy per particle of bulk symmetric matter at saturation. E_S, E_C, $E_{\rm dif}$, and E_{ex} correspond to the surface energy of symmetric matter, the Coulomb energy of a uniformly charged sphere, the diffuseness correction, and the exchange correction to the Coulomb energy, respectively. The last term gives the pairing correction, Δ is a constant, and $a = +1$ for odd-odd nuclei, 0 for odd-even, and -1 for even-even nuclei. $S(A)$ is the symmetry energy expressed by the volume $S^V(A)$ and modified surface component $S^S(A)$ in the droplet model (see Ref. [38], where it is defined as S_s^*):

$$S(A) = \frac{S^V(A)}{1+\frac{S^S(A)}{S^V(A)}A^{-1/3}} = \frac{S^V(A)}{1+q(A)A^{-1/3}}, \quad (2)$$

where

$$q(A) \equiv \frac{S^S(A)}{S^V(A)}. \quad (3)$$

We note that, in the present work, we use Eq. (2) as a basic relation between the symmetry energy $S(A)$ and its volume $S^V(A)$ and surface $S^S(A)$ components. The reason we use Eq. (2) in contrast with the relation in another approach used in, e.g., Refs. [39–42], and also in our work [31], was discussed in detail in our previous work [9]. It is motivated by the necessity to have a correct behavior of the denominator in Eq. (2) in the infinite-nuclear-matter limit. More precisely, in the limit $A \to \infty$ the ratio in Eq. (2), $S^S/S^V \to 0$, so that $[S^S/S^V]A^{-1/3} \to 0$ and the symmetry energy in Eq. (2) has the correct limit $S \to S^V$. Contrary to this, in the approach of Refs. [39–42] in the limit $A \to \infty$ the term $[S^V(A)/S^S(A)]A^{-1/3}$ is not well determined. The use of the latter approach needs a condition to be imposed, namely, the surface coefficient $S^S(A)$ to go to zero more slowly than $A^{-1/3}$ as $A \to \infty$. This is the reason why we use in our work Eq. (2) instead of the relation in the approach in, e.g., Refs. [39–42].

At very large A we may write the symmetry energy in the known form (see Ref. [36]):

$$S(A) \simeq S^V(A) - \frac{S^S(A)}{A^{1/3}}, \quad (4)$$

which follows from Eq. (2) for large A.

The relations of $S^V(A)$ and $S^S(A)$ with $S(A)$ in terms of $q(A)$ can be found from Eqs. (2) and (3):

$$S^V(A) = S(A)\left[1+\frac{q(A)}{A^{1/3}}\right], \quad (5)$$

$$S^S(A) = q(A)S(A)\left[1+\frac{q(A)}{A^{1/3}}\right]. \quad (6)$$

The following expression for the ratio of the volume to the surface symmetry energy coefficients was given by Danielewicz [39] (see also Ref. [43]):

$$\kappa(A) = \frac{S^V(A)}{S^S(A)} = \frac{3}{r_0}\int dr\frac{\rho(r)}{\rho_0}\left\{\frac{S^{NM}(\rho_0)}{S^{NM}[\rho(r)]} - 1\right\}, \quad (7)$$

where $S^{NM}[\rho(r)]$ is the nuclear matter symmetry energy, $\rho(r)$ is the half-infinite nuclear matter density, ρ_0 is the nuclear matter equilibrium density, and r_0 is the radius of the nuclear volume per nucleon. The latter two quantities are related by

$$\frac{4\pi r_0^3}{3} = \frac{1}{\rho_0}. \quad (8)$$

Here we give for completeness the following general expression for the nuclear matter symmetry energy used in Eq. (7):

$$S^{NM}(\rho) = \frac{1}{2}\frac{\partial^2 E(\rho,\delta)}{\partial\delta^2}\bigg|_{\delta=0} = a_4 + \frac{p_0^{NM}}{\rho_0^2}(\rho-\rho_0) + \frac{\Delta K^{NM}}{18\rho_0^2}(\rho-\rho_0)^2 + \cdots, \quad (9)$$

where $E(\rho,\delta)$ is the energy per particle for nuclear matter that depends on the density and the isospin asymmetry $\delta = (\rho_n - \rho_p)/\rho$ with the baryon density $\rho = \rho_n + \rho_p$, ρ_n and ρ_p being the neutron and proton densities. The parameter a_4 is the symmetry energy at equilibrium [$a_4 = S^{NM}(\rho_0)$], while the pressure p_0^{NM} and the curvature ΔK^{NM} have the corresponding forms:

$$p_0^{NM} = \rho_0^2\frac{\partial S^{NM}}{\partial\rho}\bigg|_{\rho=\rho_0}, \quad (10)$$

$$\Delta K^{NM} = 9\rho_0^2\frac{\partial^2 S^{NM}}{\partial\rho^2}\bigg|_{\rho=\rho_0}. \quad (11)$$

In the next two sections we present our relationships for the ratio of $S^V(A)$ and $S^S(A)$ obtained in the approaches considered within the framework of the coherent density fluctuation model [9–11,31]. Our results for the mentioned quantities are given in Sec. III.

B. Equation-of-state parameters of finite nuclei in the coherent density fluctuation model

In the present work we calculate the EOS parameters in finite nuclei, such as the nuclear symmetry energy and its surface and volume components, by using the CDFM. As mentioned in the introduction, the model is based on the δ-function limit of the generator coordinate method [11,14]; it is a natural extension of the Fermi-gas model and includes NN correlations of collective type. An important feature of the CDFM is that it allows us to make the transition from nuclear matter quantities to the corresponding quantities in finite nuclei. In the CDFM, the one-body density matrix $\rho(\mathbf{r},\mathbf{r}')$ is a coherent superposition of the one-body density matrices $\rho_x^{NM}(\mathbf{r},\mathbf{r}')$ for spherical "pieces" of nuclear matter ("fluctons") with radius x and density $\rho_x(\mathbf{r}) = \rho_0(x)\Theta(x-|\mathbf{r}|)$, where

$$\rho_0(x) = \frac{3A}{4\pi x^3}, \quad (12)$$

in which all A nucleons are homogeneously distributed:

$$\rho_x^{NM}(\mathbf{r},\mathbf{r}') = 3\rho_0(x)\frac{j_1(k_F(x)|\mathbf{r}-\mathbf{r}'|)}{(k_F(x)|\mathbf{r}-\mathbf{r}'|)} \Theta\left(x-\frac{|\mathbf{r}+\mathbf{r}'|}{2}\right). \quad (13)$$

It has the form

$$\rho(\mathbf{r},\mathbf{r}') = \int_0^\infty dx|F(x)|^2\rho_x^{NM}(\mathbf{r},\mathbf{r}'). \quad (14)$$

In Eq. (13), j_1 is the first-order spherical Bessel function and

$$k_F(x) = \left(\frac{3\pi^2}{2}\rho_0(x)\right)^{1/3} \equiv \frac{\beta}{x}, \quad (15)$$

with

$$\beta = \left(\frac{9\pi A}{8}\right)^{1/3} \simeq 1.52A^{1/3} \quad (16)$$

being the Fermi momentum of the nucleons in the flucton. The nucleon density distribution in the CDFM has the form:

$$\rho(\mathbf{r}) = \int_0^\infty dx|F(x)|^2\rho_0(x)\Theta(x-|\mathbf{r}|). \quad (17)$$

It can be seen from Eq. (17) that, in the case of monotonically decreasing local density ($d\rho/dr \leqslant 0$), the weight function $|F(x)|^2$ can be obtained from a known density (obtained theoretically or experimentally):

$$|F(x)|^2 = -\frac{1}{\rho_0(x)}\frac{d\rho(r)}{dr}\bigg|_{r=x}. \quad (18)$$

It has been shown in our previous works [8,29,31] that the following expression for the nuclear symmetry energy in finite nuclei $S(A)$ can be obtained within the CDFM on the base of the infinite matter one $S^{NM}(\rho)$ (at temperature $T = 0$ MeV) by weighting it with $|F(x)|^2$:

$$S(A) = \int_0^\infty dx|F(x)|^2 S^{NM}[\rho(x)]. \quad (19)$$

Here we would like to note that, when our procedure is applied to quantities of (infinite) nuclear matter, the self-consistency requires the weight function to reduce to the Dirac δ function. For instance, when the self-consistency is applied to the density $\rho(|\mathbf{r}|)$ and the symmetry energy $S^{NM}[\rho(|\mathbf{r}|)]$ in nuclear matter it leads from Eqs. (17) and (19) to the identities

$$\rho^{NM}(|\mathbf{r}|,x) = \int_0^\infty dx'\delta(x'-x)\rho_0(x')\Theta(x'-|\mathbf{r}|) = \rho_0(x)\Theta(x-|\mathbf{r}|), \quad (20)$$

$$S^{NM}[\rho^{NM}(|\mathbf{r}|,x)] = \int_0^\infty dx'\delta(x'-x)S^{NM}[\rho^{NM}(|\mathbf{r}|,x')] = S^{NM}[\rho_0(x)\Theta(x-|\mathbf{r}|)]. \quad (21)$$

In our already mentioned works (including Ref. [9]) we applied the CDFM in the framework of the self-consistent Skyrme-Hartree-Fock plus BCS method to calculate the volume and surface components of the symmetry energy and their ratio in the Ni, Sn, and Pb isotopic chains. In our first scheme to calculate the ratio $\kappa(A)$ we started from the expression of Eq. (7) (see, e.g., Refs. [39,43]) making in it a preliminary assumption replacing the density $\rho(r)$ for the half-infinite nuclear matter in the integrand by the density distribution of a finite nucleus, namely, by the expression in the CDFM [Eq. (17)]. Following the procedure whose details are given in our work [9] and using Eqs. (20) and (21), we obtain the formula for $\kappa(A)$ in the form

$$\kappa(A) = \frac{3}{r_0\rho_0}\int_0^\infty dx|\mathcal{F}(x)|^2\rho_0(x) \times \int_0^x dr\left\{\frac{S^{NM}(\rho_0)}{S^{NM}[\rho_0(x)]}-1\right\}, \quad (22)$$

which leads finally to

$$\kappa(A) = \frac{3}{r_0\rho_0}\int_0^\infty dx|\mathcal{F}(x)|^2 x\rho_0(x)\left\{\frac{S^{NM}(\rho_0)}{S^{NM}[\rho_0(x)]}-1\right\}. \quad (23)$$

The right-hand side of Eq. (23) is an one-dimensional integral over x, the latter being the radius of the "flucton" that is perpendicular to the nuclear surface. We refer to the expression in Eq. (23) as scheme I, because this was the first equation that we used for the numerical calculations of the results presented in Refs. [9,31]. We note that a careful analysis of the integration interval in Eq. (23) required in order to avoid possible singularities in the integrand in some x ranges was carried out in our previous works.

C. An alternative approach in the coherent density fluctuation model to calculate the ratio of surface-to-volume components of the nuclear symmetry energy

As mentioned in the introduction, the main aim in the present work is to provide an alternate scheme to calculate the ratio $q(A)$ as defined in Eq. (3). Here we would like to underline the main differences in the construction of scheme II in comparison with the previous scheme I: (i) we do not use the method in Refs. [39,43], and (ii) we avoid the above-mentioned assumption in Sec. II B, namely, the replacement of the density $\rho(r)$ for the half-infinite nuclear matter by the density distribution of a finite nucleus. A third and important reason to choose a different scheme is that the integrand in Eq. (23) for κ in scheme I presents singularities for some of the potentials (e.g., for the Brueckner potential). Thus, the results for κ become extremely sensitive to the choice of the integration interval, mainly to the value of the lower limit of integration in Eq. (23). In the proposed scheme II we start from the general relationship [Eq. (2)] between the NSE S and its components S^V and S^S. The procedure of the derivation of $q(A)$ for finite nuclei is as follows: (i) we determine the ratio $q(x) = S^S(x)/S^V(x)$ for the "fluctons" of the CDFM from the basic Eqs. (2) and (4), and (ii) we construct $q(A)$ within the CDFM rules weighting $q(x)$ by the weight function $|F(x)|^2$. First, to construct $q(x) = S^S(x)/S^V(x)$ in the x-flucton we recall that the x-flucton is a sphere of nuclear matter of radius x with density $\rho_0(x)$. This implies that inside each flucton we may apply Eq. (4) in the form $S^S/S^V \simeq (1 - S/S^V)A^{1/3}$, with A being the number of nucleons in the flucton and given by $(x/r_0)^3[\rho_0(x)/\rho_0]$

[see Eqs. (8) and (12)], and S being the nuclear matter symmetry energy in the flucton $[S^{NM}(\rho_0(x))]$ with volume component $S^V \simeq S^{NM}(\rho_0)$. This results in the following expression for $q(x)$:

$$q(x) = \frac{S^S(x)}{S^V(x)} = \frac{x}{r_0}\left[\frac{\rho_0(x)}{\rho_0}\right]^{1/3}\left[1 - \frac{S^{NM}[\rho_0(x)]}{S^{NM}(\rho_0)}\right]. \quad (24)$$

Weighting $q(x)$ by the function $|F(x)|^2$ leads to the following relationship for the ratio (3):

$$q(A) = \int_0^\infty dx|F(x)|^2 q(x) = \int_0^\infty dx|F(x)|^2 \times \frac{x}{r_0}\left[\frac{\rho_0(x)}{\rho_0}\right]^{1/3}\left[1 - \frac{S^{NM}[\rho_0(x)]}{S^{NM}(\rho_0)}\right]. \quad (25)$$

We refer to the expression in Eq. (25) as scheme II. Here we would like to note the following: (i) the expression (24) for a flucton is obtained in a direct and natural way starting from the known formula (4) that follows from the general relationship (2) at large A. (ii) Equation (25) is obtained without preliminary assumptions that were imposed to obtain Eq. (23) in scheme I and is free from singularities. (iii) As a result of (i) and (ii) the calculated quantity $1/q = S^V/S^S$ that follows from Eq. (25) is not equal to the previously calculated quantity κ following Eq. (23). We note that both quantities are obtained within different schemes, although both are within the framework of the CDFM. Of course, the values of the results for $1/q(A)$ coming from Eq. (25) and $\kappa(A)$ [Eq. (23)] can be compared and this is done in the next section, analyzing in this way the role of the assumptions made in approach I and the proposed direct CDFM scheme II (the latter being without extra assumptions and free from singularities) on the studied quantities.

In the next Sec. III we present our results for the proposed ratio $q(A)$ as well as the new CDFM results for the symmetry energy components $S^V(A)$ [Eq. (5)] and $S^S(A)$ [Eq. (6)] in terms of $S(A)$ [Eq. (19)] and $q(A)$ [Eq. (25)], in comparison with our previous results for the corresponding quantities in the case of the three isotopic chains of Ni, Sn, and Pb using Skyrme, Bruckner, Bonn B, and Bonn CD potentials. The self-consistent Skyrme-HF plus BCS method is used in the calculations of the nuclear densities of these nuclei and the CDFM weight function $|F(x)|^2$. The results for the ratio $1/q$ are presented and discussed in relation to the values of κ and compared with the available empirical data and with results of other theoretical considerations.

III. RESULTS AND DISCUSSION

As the main emphasis of the present study is to propose a different approach to study the nuclear symmetry energy components and their ratio, we start our analysis with the two basic quantities entering the integrands in Eq. (25) for the ratio $q(A)$, namely, the symmetry energy of nuclear matter $S^{NM}[\rho_0(x)]$ in a flucton with density $\rho_0(x)$ and the weight function $|F(x)|^2$. Then, obtaining the symmetry energy in finite nuclei within the CDFM from Eq. (19) its volume and surface components in the proposed approach can be calculated from Eqs. (5) and (6), respectively.

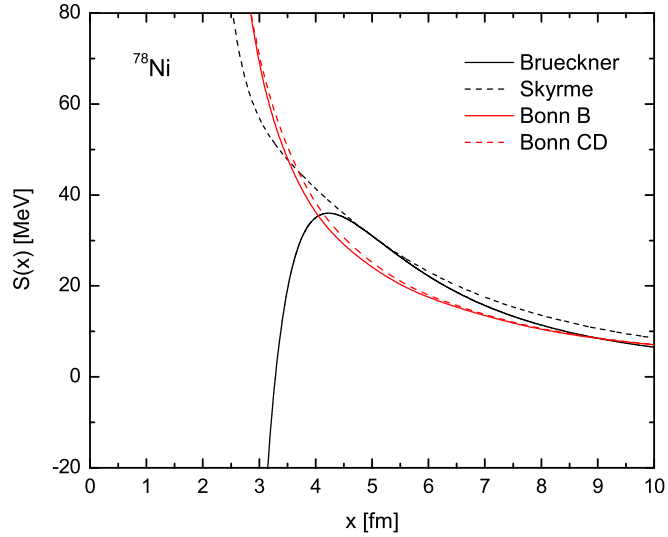

FIG. 1. The symmetry energy $S(x)$ of the double-magic nucleus ^{78}Ni as a function of the flucton radius x [related to its density $\rho_0(x) = 3A/(4\pi x^3)$] calculated with the Brueckner EDF (black solid line), Skyrme EDF (black dashed line), and the BHF method with the Bonn B (red solid line) and Bonn CD (red dashed line) potentials from Refs. [44,45].

As an example, we show first in Fig. 1 the results for the symmetry energy $S(x)$ of the double-magic nucleus ^{78}Ni corresponding to nonrelativistic BHF results with realistic Bonn B and Bonn CD potentials as well as to the Brueckner and Skyrme EDFs, for which analytical expressions for $S^{NM}(x)$ can be found in Refs. [8,29–31]. As can be seen in Fig. 1, the symmetry energy derived from the energy density functional of Brueckner *et al.* [6,7] goes extremely low below $x = 4$ fm in comparison with the other three cases. The latter exhibit a smooth behavior and their corresponding curves are close to each other. The Brueckner symmetry energy curve behaves similarly to them in the range $x > 4$ fm. The reason for the particular behavior of $S(x)$ in the case of Brueckner EDF lies in its parametrization as a function of the density performed in nuclear matter calculations. The symmetry energy versus x plotted in Fig. 1 corresponds to the Brueckner curve displayed in Fig. 5 of Ref. [9], where the symmetry energy is given versus the density ρ, as follows: the region $x \leqslant 4$ fm corresponds to the right "wing" after the maximum of $S^{NM}(\rho)$ at around $\rho = 0.24$ fm^{-3} (see Fig. 5 of Ref. [9]), while the region $x > 4$ fm refers to the left "wing" before the maximum. The behavior of $S(x)$ in the case of the Brueckner EDF shows its isospin instability. Due to this fact, a lower cutoff is needed to compute Eqs. (19) and (25), but this is naturally supplied by the function $|F(x)|^2$ as explained in the discussions that follow. Here we should note that the observed differences of the symmetry energy at $x < 4$ fm in the particular case of ^{78}Ni (see Fig. 1) provide us with a hint about the range of the lower limit of integration in Eq. (25) in order to get correct physical values for the ratio of the surface-to-volume components of the nuclear symmetry energy.

In Fig. 2 are given the CDFM weight functions $|F(x)|^2$ of double-magic ^{78}Ni, ^{132}Sn, and ^{208}Pb nuclei as a function of the

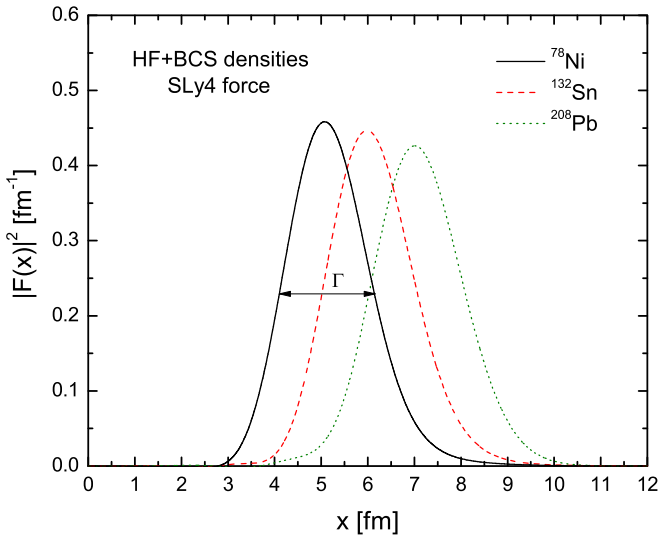

FIG. 2. The weight functions $|F(x)|^2$ [Eq. (18)] of double-magic ^{78}Ni, ^{132}Sn, and ^{208}Pb nuclei calculated in the Skyrme HF+BCS method with the SLy4 force.

fluction radius x. Their densities are obtained in self-consistent HF+BCS calculations with SLy4 interaction [46]. The function $|F(x)|^2$ which is used in Eqs. (19), (23), and (25) has the form of a bell with a maximum around $x = R_{1/2}$ at which the value of the density $\rho(x = R_{1/2})$ is around half of the value of the central density equal to $\rho_c[\rho(R_{1/2})/\rho_c = 0.5]$. Namely, in this region around $\rho = \rho_c/2$ the values of different $S^{NM}(\rho)$ play the main role in the calculations. Therefore, to fully specify the role of both quantities $S^{NM}[\rho_0(x)]$ and $|F(x)|^2$ in the expression (25) for the ratio $q(A)$ and to determine the relevant region of densities in finite nucleus calculations, we apply a physical criterion related to the weight function $|F(x)|^2$. The latter contains the nuclear structure information through the total nuclear density. In this respect, the width Γ of the weight function $|F(x)|^2$ at its half maximum (which is illustrated in Fig. 2 on the example of ^{78}Ni nucleus) is a good and acceptable choice.

As known, the central density of the nucleus has values around $\rho_c \approx 0.10$–0.16 fm^{-3}. Consequently, the maximum of the weight function $|F(x)|^2$ is around $\rho(R_{1/2}) \approx 0.05$–$0.08$ fm^{-3}. In the case of ^{78}Ni (see Fig. 6 in Ref. [9]) the maximum of $|F(x)|^2$ is at $\rho = 0.05$ fm^{-3} and, within its width range, the density ρ is between 0.12 and 0.01 fm^{-3}. Thus, from the combined analysis of $S^{NM}(\rho)$ and $|F(x)|^2$ it turns out that the relevant values of the NM symmetry energy are typically those in the region around $\rho \approx 0.01$–0.12 fm^{-3} (see also the discussion in Ref. [9]). More specifically, within the proposed approach we define the lower limit of integration as the lower value of the radius x, corresponding to the left point of the half-width Γ. To test the sensitivity of this criterion, we perform additional calculations taking $\Gamma \pm 10\%$. In this case, the results for the ratio $1/q$ of a given nucleus displayed a very small sensitivity in the case of Bonn B and Bonn CD potentials, while in the case of Brueckner and Skyrme EDFs the results when applying criteria related to Γ and $\Gamma \pm 10\%$ are almost identical. We also note that, in the proposed scheme, there are no singularities in the integrand of Eq. (25) as those mentioned for the integrand of Eq. (23).

Next, we show in Fig. 3 the results of the calculations following from Eq. (25) of the ratio $1/q = S^V/S^S$ as a function of the mass number A for the isotopic chains of Ni, Sn, and Pb with SLy4 force. In Table I the values of this ratio obtained within the new scheme are compared with the values of κ [Eq. (23)] calculated from our previous scheme within the CDFM [9,31]. We would like to emphasize that this comparison is between quantities obtained in two different CDFM schemes and it can serve basically to show the influence and the importance of the preliminary assumptions and shortcomings made of scheme I and the advantage of the new scheme that is free from them.

In general, the values of $1/q$ within the new CDFM scheme calculated using the Skyrme EDF for the isotopic chains of Ni, Sn, and Pb are between 1.70 and 2.40. This range of values is similar to the estimations for $\kappa(A)$ [Eq. (23)] of Danielewicz *et al.* obtained from a wide range of available data on the binding energies [41], of Steiner *et al.* [38], and from a fit to other nuclear properties, such as the excitation energies to IAS and skins [40] $2.6 \leqslant \kappa \leqslant 3.0$ and from masses and skins [40] $2.0 \leqslant \kappa \leqslant 2.8$.

The values of $1/q$ obtained using the Brueckner EDF for the Ni isotopic chain with SLy4 force are in agreement partly with that obtained in Ref. [43] by Dieperink and Van Isacker from the analyses of masses and skins $1.6 \leqslant \kappa \leqslant 2.0$. The obtained values of $1/q$ for Sn and Pb isotopes using the Brueckner EDF together with those when using both Bonn potentials are close to the value of 1.14 given by Bethe in Ref. [36] and to the estimated value of 1.1838 by Myers and Swiatecki [37]. Generally, we can note that the results of the new scheme for $1/q$, in particular using Skyrme and Brueckner EDFs, cover reasonably the estimated values of κ (between 1.14 and 2.80) in a better way than in the previous scheme.

Here we note the observed peaks in the ratio $1/q$ at $A = 78$ and $A = 132$ for Ni and Sn isotopes, respectively. They are more pronounced for the choice of the Skyrme EDF, less pronounced for Brueckner EDF, and are somewhat smoothed out for Bonn B and Bonn CD potentials. We attribute these peaks to the sharp nuclear density transition when passing double-magic nuclei, such as ^{78}Ni and ^{132}Sn, in an isotopic chain. The peculiarities of $\rho(r)$ (and consequently the derivative of $\rho(r)$ which determines the weight function $|F(x)|^2$) for the closed shells lead to the existence of "kinks" that had been found and discussed in our previous works [8,9,29,31,32]. In the case of Pb isotopic chain (see Fig. 3) such kink does not exist at $A = 208$ and this reflects the smooth behavior without kinks of $S(A)$ [Eq. (19)] and related quantities for the Pb isotopic chain [8,29]. Similar peaks in the ratio κ as a function of the mass number have been observed in our previous studies [9,31].

The values of the symmetry energy S [Eq. (19)] and its volume S^V [Eq. (5)] and surface S^S [Eq. (6)] components as functions of A deduced within the proposed scheme for the same isotopic chains are presented in Fig. 4. The calculated symmetry energy for the three isotopic chains and all considered potentials turns out to be between 24 and 31 MeV

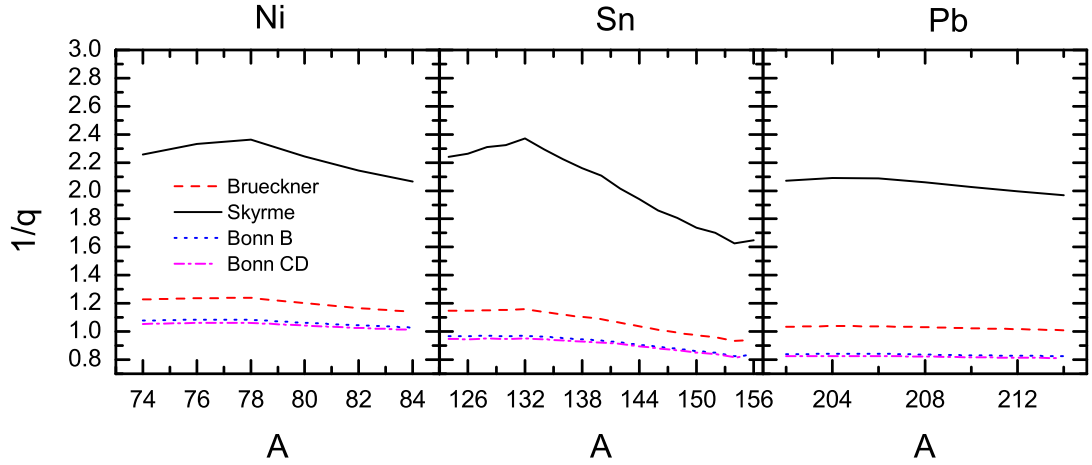

FIG. 3. The quantity $1/q = S^V/S^S$ [following from Eq. (25)] as a function of A for the isotopic chains of Ni, Sn, and Pb obtained using Brueckner EDF (dashed line), Skyrme EDF (solid line), and BHF method with Bonn B (dotted line) and Bonn CD (dash-dotted line) potentials from Refs. [44,45]. The weight function $|F(x)|^2$ [Eq. (18)] used in the calculations is obtained by means of the densities derived within a self-consistent Skyrme-Hartree-Fock plus BCS method with the SLy4 force.

(see Fig. 4). In practice, predictions for the symmetry energy vary substantially (28–38 MeV), e.g., an empirical value of the symmetry energy 30 ± 4 MeV is given in Refs. [47,48]. The values of the volume contribution S^V to the NSE obtained within the new scheme in the case of Brueckner and Skyrme EDFs are smaller than those derived from the previous CDFM scheme I (presented in Tables I and III of Ref. [31]). We would like to emphasize that the results for S^V in the scheme II (between 29 and 34 MeV) are more realistic than those previously obtained within our scheme I, for instance, using Brueckner EDF (between 41.5 and 43 MeV). The new results with scheme II are in good agreement with the available phenomenological estimations, as follows: Ref. [40]: $30.0 \leqslant S^V \leqslant 32.5$ MeV, Ref. [42]: $31.5 \leqslant S^V \leqslant 33.5$ MeV. In the case of Ni isotopic chain our previous calculations [9] with SLy4 force provided values of the volume symmetry energy within 27.6 and 28.1 MeV for the Bonn B potential and within 28.4–29.1 MeV for the Bonn CD potential. In the proposed approach for the same potentials the corresponding values of S^V are larger by 2 MeV and are better compared with the results presented in Refs. [40,42]. Concerning the surface component of the NSE, S^S, it is known that this component is poorly constrained by empirical data. Therefore, it is useful to test different EDFs and nuclear potentials within different approaches to collect more information about it. Figure 4 shows that the range of the values obtained for S^S and for Ni, Sn, and Pb isotopes in the case of Skyrme EDF is 14–18 MeV. These results come closer to the limits on the surface symmetry parameter 11 MeV $\leqslant \beta \leqslant$ 14 MeV established in Ref. [41]. The proposed CDFM scheme gives larger values for the surface component in the case of the three other potentials (Brueckner, Bonn B, and Bonn CD).

We would like to note that the same peculiarities (as for the ratio $1/q = S^V/S^S$ presented in Fig. 3), namely, "kinks," appear in the cases of S, S^V, and S^S as functions of the mass number A at the double-magic ^{78}Ni and ^{132}Sn isotopes. They are stronger or weaker and depending on the use of a given nuclear potential. In Fig. 4 a kink appears for $S(A)$ and $S^V(A)$ not only for the double-magic ^{132}Sn but also for the semimagic ^{140}Sn nucleus. As was discussed in Ref. [31], the latter is related to the closed $2f_{7/2}$ subshell for neutrons. Kinks of the A dependence of the symmetry energy and its components in the Pb isotopic chain are not observed.

To summarize this section, we would like to stress that the comparison of the results of the proposed scheme II with those of scheme I is mainly informative to test the role of the approximations in scheme I versus the proposed procedure in scheme II that is free from them. This comparison together with the comparison with phenomenological estimates of the

TABLE I. The ranges of changes of $1/q$ (scheme II) and κ (scheme I) [9,31] with Skyrme and Brueckner EDFs and the BHF method with Bonn B and Bonn CD potentials for Ni, Sn, and Pb isotopic chains.

	Ni		Sn		Pb	
	$1/q$	κ	$1/q$	κ	$1/q$	κ
Skyrme	2.07–2.36	1.53–1.70	1.63–2.37	1.58–2.02	1.97–2.09	1.67–1.71
Brueckner	1.14–1.24	2.22–2.44	0.94–1.16	2.40–2.90	1.01–1.04	2.62–2.64
Bonn B	1.03–1.08	1.80–1.90	0.83–0.97	2.00–2.48	0.84–0.88	2.54–2.80
Bonn CD	1.01–1.06	1.80–2.00	0.82–0.95	2.00–2.48	0.81–0.83	2.54–2.80

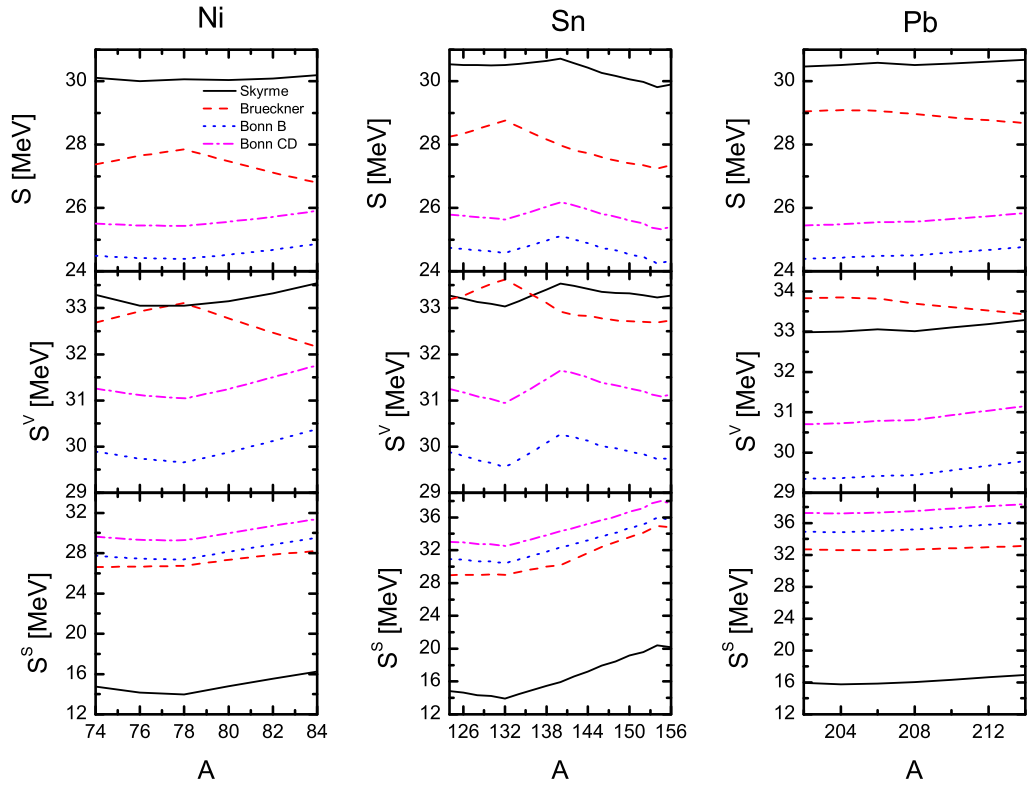

FIG. 4. The symmetry energy S [Eq. (19)] and its volume S^V [Eq. (5)] and surface S^S [Eq. (6)] components for the isotopic chains of Ni, Sn, and Pb obtained using Brueckner EDF (dashed line), Skyrme EDF (solid line), and BHF method with Bonn B (dotted line) and Bonn CD (dash-dotted line) potentials from Refs. [44,45]. The weight function $|F(x)|^2$ [Eq. (18)] used in the calculations is obtained by means of the densities derived within a self-consistent Skyrme-Hartree-Fock plus BCS method with SLy4 force.

NSE components, mainly the volume component, allows us to conclude that the results of scheme II are more realistic.

IV. SUMMARY AND CONCLUSIONS

The results of the present work can be summarized as follows:

(i) We provide an alternative approach (scheme II) to calculate the ratio $q(A) = S^S(A)/S^V(A)$ of the surface-to-volume components of the NSE within the framework of the CDFM in a more direct and simple way and having stronger physical grounds than the former one (scheme I) that had been used in our previous works [9,31]. In the proposed approach we first determine the ratio $q(x)$ for a fluctuon in the CDFM model from the basic droplet model mass formula and then we use the convolution of $q(x)$ with $|F(x)|^2$ to construct $q(A)$ for finite nuclei following the standard CDFM procedure. In this way the proposed scheme avoids some conceptual and mathematical shortcomings that were met in the previous scheme.

(ii) The results for $q(A)$ and the components $S^S(A)$ and $S^V(A)$ are obtained from calculations based on Skyrme and Brueckner energy-density functionals for nuclear matter and nonrelativistic Brueckner-Hartree-Fock method with realistic Bonn B and Bonn CD NN potentials. As in our previous scheme, by applying the CDFM the finite nuclei densities from the isotopic chains of Ni, Sn, and Pb are obtained in self-consistent Hartree-Fock+BCS calculations with SLy4 Skyrme effective interaction.

(iii) We would like to note the dependence of the results for the ratio of S^S to S^V on the effective nuclear potentials used in the calculations. In this respect, the results of our calculations using Skyrme EDF turn out to be close to the different estimations obtained from a fit to nuclear properties, such as the excitation energies to IAS and neutron-skin thickness [40], masses, and others. The values of $1/q$ obtained using the Brueckner EDF for the Ni isotopic chain are in agreement with those obtained in Ref. [43] from the analyses of masses and skins. In the case of Bonn B and Bonn CD two-body potentials the results for the ratio $1/q$ approach the estimated values from the works of Bethe [36] and Myers and Swiatecki [37]. Overall, the results of the proposed scheme for $1/q$ cover reasonably the whole region of estimated values for κ (between 1.14 and 2.80) and in some cases are somewhat better than the values obtained in the previous scheme.

(iv) The values of the symmetry energy S for the three isotopic chains and all considered potentials are between 24 and 31 MeV, which is in accordance with the region of its empirical values 30 ± 4 MeV given in Refs. [47,48]. The results for the volume component $S^V(A)$ of NSE in scheme II (between 29 and 34 MeV) are in good agreement with those of Refs. [40,42] (between 30 and 33.5 MeV). The values of the surface contribution $S^S(A)$ in scheme II in the case of Skyrme EDF (14–18 MeV)

come closer to the region of 11–14 MeV established in Ref. [41].

(v) Analyzing the isotopic sensitivity of $S^V(A)$, $S^S(A)$, and their ratio $1/q(A)$ we observe peculiarities ("kinks") of these quantities as functions of the mass number A in the cases of the double-magic ^{78}Ni and ^{132}Sn isotopes, as well as a "kink" of $S^V(A)$ for ^{140}Sn. No pronounced peak at the double-magic nucleus with $A = 208$ in the Pb chain is found. The mentioned peculiarities in the behavior of the corresponding curves for the same quantities have been observed also in our previous CDFM scheme.

Finally, we point out that the results for the NSE components and their ratio obtained within the two CDFM schemes are comparable in many considered cases and cover a range of values that is compatible with the range of available empirical data and with other theoretical results, showing the power of the CDFM method, which includes effects of nucleon-nucleon correlations of collective type. However, we would like to emphasize that the presented comparison of the results of both schemes is informative mainly for the role of the approximations made in scheme I, while scheme II is free from those approximations and is considered to be more reliable and realistic leading to results that are in better agreement with data.

ACKNOWLEDGMENTS

A.N.A, M.K.G., and D.N.K. are grateful for the support of the Bulgarian National Science Fund under Contract No. KP-06-N38/1. I.C.D also wishes to acknowledge partial financial support from the University of Mount Olive Professional Development Fund. P.S. acknowledges support from Ministerio de Ciencia e Innovación MCIU/AEI/FEDER,UE (Spain) under Contract No. PGC2018-093636-B-I00.

[1] I. Bombaci and D. Logoteta, Astron. Astrophys. **609**, A128 (2018).
[2] A. Chbihi, M. Boisjoli, P. Marini, E. Bonnet, J. D. Frankland, D. Gruyer, and G. Verde, JPS Conf. Proc. **6**, 020052 (2015).
[3] T. Klähn *et al.*, Phys. Rev. C **74**, 035802 (2006).
[4] W. Horiuchi, S. Ebata, and K. Iida, Phys. Rev. C **96**, 035804 (2017).
[5] N. Wang, M. Liu, L. Ou, and Y. Zhang, Phys. Lett. B **751**, 553 (2015).
[6] K. A. Brueckner, J. R. Buchler, S. Jorna, and R. J. Lombard, Phys. Rev. **171**, 1188 (1968).
[7] K. A. Brueckner, J. R. Buchler, R. C. Clark, and R. J. Lombard, Phys. Rev. **181**, 1543 (1969).
[8] M. K. Gaidarov, A. N. Antonov, P. Sarriguren, and E. Moya de Guerra, Phys. Rev. C **84**, 034316 (2011).
[9] I. C. Danchev, A. N. Antonov, D. N. Kadrev, M. K. Gaidarov, P. Sarriguren, and E. Moya de Guerra, Phys. Rev. C **101**, 064315 (2020).
[10] A. N. Antonov, V. A. Nikolaev, and I. Zh. Petkov, Bulg. J. Phys. **6**, 151 (1979); Z. Phys. A **297**, 257 (1980); **304**, 239 (1982); Nuovo Cimento A **86**, 23 (1985); A. N. Antonov, E. N. Nikolov, I. Zh. Petkov, Ch. V. Christov, and P. E. Hodgson, *ibid.* **102**, 1701 (1989); A. N. Antonov, D. N. Kadrev, and P. E. Hodgson, Phys. Rev. C **50**, 164 (1994).
[11] A. N. Antonov, P. E. Hodgson, and I. Zh. Petkov, *Nucleon Momentum and Density Distributions in Nuclei* (Clarendon Press, Oxford, 1988); *Nucleon Correlations in Nuclei* (Springer-Verlag, Berlin, Heidelberg, 1993).
[12] A. Carbone, A. Polls, and A. Rios, Europhys. Lett. **97**, 22001 (2012).
[13] I. Vidaña, C. Providência, and A. Polls, Symmetry **7**, 15 (2015).
[14] J. J. Griffin and J. A. Wheeler, Phys. Rev. **108**, 311 (1957).
[15] A. N. Antonov, I. S. Bonev, Ch. V. Christov, and I. Zh. Petkov, Nuovo Cimento A **100**, 779 (1988).
[16] A. N. Antonov, V. A. Nikolaev, and I. Zh. Petkov, Bulg. J. Phys. **18**, 107 (1991).
[17] A. N. Antonov, M. K. Gaidarov, D. N. Kadrev, M. V. Ivanov, E. M. de Guerra, and J. M. Udias, Phys. Rev. C **69**, 044321 (2004).
[18] A. N. Antonov, M. K. Gaidarov, M. V. Ivanov, D. N. Kadrev, E. Moya de Guerra, P. Sarriguren, and J. M. Udias, Phys. Rev. C **71**, 014317 (2005).
[19] A. N. Antonov, M. V. Ivanov, M. K. Gaidarov, E. Moya de Guerra, P. Sarriguren, and J. M. Udias, Phys. Rev. C **73**, 047302 (2006).
[20] A. N. Antonov, M. V. Ivanov, M. K. Gaidarov, E. Moya de Guerra, J. A. Caballero, M. B. Barbaro, J. M. Udias, and P. Sarriguren, Phys. Rev. C **74**, 054603 (2006).
[21] M. V. Ivanov, M. B. Barbaro, J. A. Caballero, A. N. Antonov, E. Moya de Guerra, and M. K. Gaidarov, Phys. Rev. C **77**, 034612 (2008).
[22] A. N. Antonov, M. V. Ivanov, M. B. Barbaro, J. A. Caballero, E. Moya de Guerra, and M. K. Gaidarov, Phys. Rev. C **75**, 064617 (2007).
[23] A. N. Antonov, M. V. Ivanov, M. B. Barbaro, J. A. Caballero, and E. M. de Guerra, Phys. Rev. C **79**, 044602 (2009).
[24] J. A. Caballero, M. B. Barbaro, A. N. Antonov, M. V. Ivanov, and T. W. Donnelly, Phys. Rev. C **81**, 055502 (2010).
[25] A. N. Antonov, M. V. Ivanov, J. A. Caballero, M. B. Barbaro, J. M. Udias, E. Moya de Guerra, and T. W. Donnelly, Phys. Rev. C **83**, 045504 (2011).
[26] D. N. Kadrev, A. N. Antonov, M. V. Stoitsov, and S. S. Dimitrova, Int. J. Mod. Phys. E **5**, 717 (1996).
[27] P. Sarriguren, D. Merino, O. Moreno, E. Moya de Guerra, D. N. Kadrev, A. N. Antonov, and M. K. Gaidarov, Phys. Rev. C **99**, 034325 (2019).
[28] B. Hernández, P. Sarriguren, O. Moreno, E. Moya de Guerra, D. N. Kadrev, and A. N. Antonov, Phys. Rev. C **103**, 014303 (2021).
[29] M. K. Gaidarov, A. N. Antonov, P. Sarriguren, and E. M. de Guerra, Phys. Rev. C **85**, 064319 (2012).
[30] M. K. Gaidarov, P. Sarriguren, A. N. Antonov, and E. Moya de Guerra, Phys. Rev. C **89**, 064301 (2014).
[31] A. N. Antonov, M. K. Gaidarov, P. Sarriguren, and E. Moya de Guerra, Phys. Rev. C **94**, 014319 (2016).
[32] A. N. Antonov, D. N. Kadrev, M. K. Gaidarov, P. Sarriguren, and E. Moya de Guerra, Phys. Rev. C **98**, 054315 (2018).

[33] M. K. Gaidarov, I. Moumene, A. N. Antonov, D. N. Kadrev, P. Sarriguren, and E. Moya de Guerra, Nucl. Phys. A **1004**, 122061 (2020).
[34] M. K. Gaidarov, A. N. Antonov, D. N. Kadrev, P. Sarriguren, and E. M. de Guerra, Chapter in *Nuclear Structure Physics*, edited by A. Shukla and S. K. Patra (CRC Press, Taylor & Francis Group, 2020), pp. 93–120.
[35] C. F. von Weizsäcker, Eur. Phys. J. A **96**, 431 (1935).
[36] H. A. Bethe, in *Theory of Nuclear Matter*, Annual Review of Nuclear Science (Palo Alto, California, USA, 1971), Vol. 21, p. 93.
[37] W. D. Myers and W. J. Swiatecki, Nucl. Phys. **81**, 1 (1966).
[38] A. W. Steiner, M. Prakash, J. M. Lattimer, and P. J. Ellis, Phys. Rep. **411**, 325 (2005).
[39] P. Danielewicz, arXiv:nucl-th/0607030.
[40] P. Danielewicz, arXiv:nucl-th/0411115.
[41] P. Danielewicz, Nucl. Phys. A **727**, 233 (2003).
[42] P. Danielewicz and J. Lee, Nucl. Phys. A **818**, 36 (2009).
[43] A. E. L. Dieperink and P. Van Isacker, Eur. Phys. J. A **32**, 11 (2007).
[44] R. Machleidt, Adv. Nucl. Phys. **19**, 189 (1989).
[45] R. Machleidt, Phys. Rev. C **63**, 024001 (2001).
[46] E. Chabanat, P. Bonche, P. Haensel, J. Meyer, and R. Schaeffer, Nucl. Phys. A **635**, 231 (1998).
[47] P. E. Haustein, At. Data Nucl. Data Tables **39**, 185 (1988).
[48] N. Nikolov, N. Schunck, W. Nazarewich, M. Bender, and J. Pei, Phys. Rev. C **83**, 034305 (2011).